Published in final edited form as:
Mol Cancer Ther. 2014 October ; 13(10): 2276–2287. doi:10.1158/1535-7163.MCT-14-0043.

Drug Repurposing Identifies a Synergistic Combination Therapy with Imatinib Mesylate for Gastrointestinal Stromal Tumor

Ziyan Y. Pessetto[1,*], **Yan Ma**[1,*], **Jeff J. Hirst**[1], **Margaret von Mehren**[2], **Scott J. Weir**[3,4,5], and **Andrew K. Godwin**[1,5]

[1]Pathology & Laboratory Medicine, University of Kansas Medical Center, Kansas City, Kansas

[2]Fox Chase Cancer Center, Philadelphia, PA

[3]Department of Pharmacology, Toxicology and Therapeutics, University of Kansas Medical Center, Kansas City, Kansas

[4]Institute for Advancing Medical Innovation, University of Kansas Medical Center, Kansas City, Kansas

[5]University of Kansas Cancer Center, Kansas City, Kansas

Abstract

Gastrointestinal Stromal Tumor (GIST) is a rare and therefore often neglected disease. Introduction of the kinase inhibitor, imatinib mesylate (IM) radically improved the clinical response of patients with GIST; however, its effects are often short-lived, with GISTs demonstrating a median time to progression of approximately two years. Although many investigational drugs, approved first for other cancers, have been subsequently evaluated for the management of GIST, few have greatly impacted the overall survival of patients with advanced disease. We employed a novel, focused, drug repurposing effort for GIST including IM-resistant GIST evaluating a large library of FDA-approved drugs regardless of current indication. As a result of the drug repurposing screen, we identified eight FDA-approved drugs including fludarabine phosphate (F-AMP) that showed synergy with and/or overcame resistance to IM. F-AMP induces DNA damage, annexin V and caspase 3/7 activities as the cytotoxic effects on GIST cells, including IM-resistant GIST cells. F-AMP and IM combination treatment showed greater inhibition of GIST cell proliferation when compared to IM alone and F-AMP alone. Successful *in vivo* experiments confirmed the combination of IM with F-AMP enhanced the antitumor effects compared to IM alone. Our results identified F-AMP as a promising, repurposed drug therapy for the treatment of GISTs, with potential to be administered in combination with IM or for treatment of IM-refractory tumors.

Corresponding Author: Andrew K. Godwin, PhD, University of Kansas Medical Center, 4005B Wahl Hall East, 3901 Rainbow Boulevard Kansas City, KS 66160. Phone: 913-945-6373; Fax: 913-945-6327; agodwin@kumc.edu.
*Z. Y Pessetto and Y. Ma have equally contributed to this work.

Note: Supplementary data for this article are available at Molecular Cancer Therapeutics Online (http://mct.aacrjournals.org).

Disclosure of Potential Conflicts of Interest: The authors declare no conflict of interest.

Keywords

drug repurposing; imatinib mesylate; fludarabine phosphate; gastrointestinal stromal tumors treatment; drug combination

INTRODUCTION

Rare or orphan diseases are defined in the U.S. as diseases affecting less than 200,000 patients. Although orphan diseases individually affect small groups of patients, collectively 25–30 million Americans suffer from rare diseases (1). Given the costs associated with the discovery, development, registration and commercialization of new drug treatments, it has traditionally been difficult for pharmaceutical companies to achieve an adequate return on investment for orphan diseases. As a result, today, we have over 6,000 rare diseases that lack effective treatments. Therefore, recent attention has been paid to the merits of exploring new potential uses of FDA-approved drugs, a drug development strategy termed drug repurposing. Repurposing FDA-approved drugs creates opportunities to advance promising new treatments to patients suffering from rare diseases much more quickly at substantially lower development costs (2). Most importantly, repurposing FDA-approved drugs provides treatment options for patients whose disease progresses at a rate that is incompatible with the 12–17 years required to discover, develop and commercialize new drugs.

Gastrointestinal Stromal Tumor (GIST), although considered rare, is the most common mesenchymal malignancy of the digestive tract with an estimated annual incidence of 6,000 new cases in the United States (3). Management of the disease has been transformed by the identification of activating mutations in the tyrosine kinase receptors, *KIT* and *PDGFRA*, in approximately 85% of GISTs (4–6). These discoveries have led to the unprecedented disease control of advanced GIST with the introduction of the kinase inhibitors imatinib mesylate, sunitinib malate, and regorafenib (6–22). However, the success of imatinib in GIST has been tempered by the fact that the treatment only increases the median time to tumor progression by approximately two years (6, 11–23). Therefore, it is clear that additional therapeutic approaches are needed.

We previously reported through a quantitative drug screen of FDA-approved drugs in GIST cells that four drugs, auranofin, bortezomib, idarubicin HCl, and F-AMP, demonstrated selective anticancer activity as single agents (1). Auranofin was prioritized for validation, and as a result of our previous studies, we obtained FDA clearance to proceed with a Phase I study in recurrent GIST patients (1). This drug repurposing trial will soon be underway to translate these findings to GIST patients with recurrent and metastatic disease (1). In this report, we describe how we have leveraged our previous work, focusing to identify repurposed drugs that might work in combination with IM.

MATERIALS AND METHODS

General methods

All cell proliferation and caspase 3/7 activity measurements were made on 384-well, black μClear microplates (Greiner bio-one, Germany). Cell proliferation experiments were

assessed using the CellTiter-blue® or CellTiter-glo® reagent according to the manufacturer's protocol (Promega). Fluorescence or luminescence measurements were made using the Infinite® M200 Pro plate reader (Tecan, Switzerland). Data were normalized to percentage inhibition.

All images were taken under an Eclipse 80i fluorescence microscope (Nikon, Japan) equipped with a QIClick™ digital CCD camera (QImaging, Canada). Images were acquired and analyzed by the MetaMorph Imaging System (Molecular Devices).

Chemicals and antibodies

The FDA-approved drug library contains 796 drugs with known bioavailability and safety profiles in humans were provided by the Lead Development and Optimization Shared Resource within the NCI-designated Cancer Center at the University of Kansas Medical Center. IM and F-AMP were purchased from the Selleckchem and dissolved in sterile water and DMSO prior to study, respectively. The following antibodies were used: anti-c-KIT, anti-p-c-KIT (Tyr719), anti-AKT, anti-p-AKT (Ser473) anti-p-AKT (Thr308), anti-ERK1/2, anti-p-ERK1/2 (Thr202/Tyr204), anti-cleaved caspase 3 (Cell Signaling technology); anti-β-actin (Sigma); and anti-Ki 67 (Dako).

Cell culture

Cells were cultured as described previously (1). Briefly, GIST-T1 cells (*c-KIT* exon 11 heterozygous mutation, obtained in 2006) was kindly provided by Takahiro Taguchi and maintained in DMEM containing 10% fetal bovine serum (FBS) (24). GIST 882 cells (c-*KIT* exon 13 homozygous mutation, obtained in 2002) were gifted from Jonathan A Fletcher and maintained in RPMI containing 15% fetal bovine serum (22, 25). GIST T1-10R cells, derived in Dr. Godwin's laboratory, were maintained in DMEM containing 10% FBS and supplied with 10 μmol/L IM to maintain drug resistance. IM was removed from the culture for indicated hours in experiments with GIST T1-10R cells. Hs 919.T cells were purchased from ATCC in 2012 and maintained in DMEM containing 10% FBS. All cells were supplied with 1% penicillin/streptomycin and were maintained in a 5% CO_2 atmosphere at 37 °C. Authentication for cell lines that were not purchased from ATCC was carried out by the University of Kansas Cancer Center Clinical Molecular Oncology Laboratory (KS).

High-throughput synergy screening

Screening conditions were optimized as described previously (1). Briefly, drugs or vehicle (DMSO) were preloaded by the University of Kansas High-Throughput Screen Laboratory to each well to give a final doses range from 10 μmol/L to 0.078 μmol/L (serial two-fold dilutions). Cells were aliquoted into plates with or without IM. The IM concentrations used for the combination study were: 10 nmol/L, 10 nmol/L, and 40 nmol/L for GIST-T1, GIST T1-10R, and GIST 882 cells, respectively.

Drug combination studies

Cells were seeded and allowed to attach overnight. IM and the FDA-approved drugs were archived in robotically accessible vials, to which media was added in preparation for addition to master plates by a Nimbus 96 liquid-dispensing workstation (Hamilton). Liquid

transfers to dilution and assay plates were handled using the same workstation adapted for the combination study procedure. Each 384-well master plate contained four 9 × 9 dose-matrix blocks, with eight serial two-fold dilutions (concentrations range from 7.8 nmol/L to 1 μmol/L) of the top concentration for each agent. Additional wells were reserved for untreated and vehicle treated control wells. The cytotoxicity of each drug and of their combinations was assessed by drug response curve, median-effect plot and normalized isobologram using the CalcuSyn Software (now replaced by CompuSyn). The median-dose effect is defined using the following equation:

$$\frac{f_a}{f_u}=\left(\frac{D}{D_m}\right)^m, \quad \text{(eq.1)}$$

where f_a is the fraction of cells affected by drug, f_u is the fraction of cells unaffected by drug, D is the drug concentration, D_m is the median-effect dose, and m is the slope or kinetic order (26). The combination index (CI) for each two-drug interactions is defined using the following equation:

$$CI=\frac{(D)_1}{(D_x)_1}+\frac{(D)_2}{(D_x)_2}=\frac{(D)_1}{(D_m)_1[f_a/1-f_a]^{1/m_1}}+\frac{(D)_2}{(D_m)_2[f_a/1-f_a]^{1/m_2}}, \quad \text{(eq.2)}$$

where $CI < 1, = 1, and > 1$ indicate synergism, additive effect, and antagonism, respectively. $(D_x)_1$ *or* $(D_x)_2$ is for $(D_x)_1$ *or* $(D_x)_2$ "alone" that inhibits a system *x%* (26–28).

Comet assay

GIST-T1 cells were treated for 3 hours with IM and F-AMP at 2 μmol/L and 10 μmol/L, respectively. The comet assay was performed under alkaline conditions as described by Singh *et al*. with minor modifications (29). Briefly, cells in ice-cold PBS were mixed with 0.5% low-melting-point agarose (Promega). Then, the suspensions were cast onto microscope slides pre-coated with 1% normal-melting-point agarose, and allowed to solidify at 4 °C. Solidified slides were immersed in lysis solution, followed by DNA denaturation solution, and pre-chilled TBE electrophoresis solution. Electrophoresis was conducted at 4 °C at an electric field strength of 1 volt/cm. After electrophoresis and rinse, gels were then dehydrated in cold 70% ethanol, air-dried and stained with ethidium bromide. At least 150 cells in 20 randomly selected fields were evaluated for each sample. DNA damage was graded by Tail DNA%, which is defined as Tail DNA intensity/Cell DNA intensity × 100%. Grade 0 = 0%; Grade 1 = 0–10%; Grade 2 = 10–30%; Grade 3 = 30–50%; Grade 4 > 50%. Three independent experiments were performed.

Early apoptosis assay

Cells were seeded and allowed to attach overnight. Cells were then treated with drugs for 48 h. Early apoptosis cells were detected and analyzed by the Guava Nexin® Annexin V assay kit using Guava easyCyte™ sampling flow cytometer (Millipore).

Cell viability and caspase 3/7 activity assay

Cells were plated and treated similar to the combination screening experiments at indicated concentrations. Cell viability was evaluated using CellTiter-blue reagent (Promega). After reading fluorescence, Caspase-Glo® 3/7 Assay Reagent (Promega) was used according to manufacturer's instructions. After background subtraction, the caspase 3/7 activities were normalized with cell viability and expressed as fold changes to the relative vehicle controls.

Western blot analysis

Cells were seeded and allowed to attach overnight. Then, cells were treated with drugs at indicated doses for 6 hours. Whole-cell extracts were prepared as described previously (18). Briefly, for each specimen, 50 μg of whole-cell extract was electrophoresed on 10% precast polyacrylamide gel (Bio-Rad) and transferred onto nitrocellulose membranes. After blocking, membranes were incubated with primary antibodies overnight at 4 °C. After incubation with HRP-conjugated secondary antibody at room temperature, development was carried out using Immun-Star™ HRP Chemiluminescence Kits (Bio-Rad).

In Vivo xenograft mouse model

All procedures were performed following the guidelines adopted by the Animal Care and Use Committee of the University of Kansas Medical Center. Female athymic nude mice (NCr-*nu*/*nu*, 5 weeks old) were purchased from the National Cancer Institute (Frederick). Three million GIST-T1 cells in PBS, mixed with an equal volume of cold BD Matrigel™ Matrix High Concentration (BD Biosciences), were inoculated subcutaneously into the right flank of each mouse. When tumor volume reached 316 mm^3 on average, mice were randomly assigned to 6 treatment groups and were treated as follows: 1) control (n=8), saline and 5% DMSO, oral gavage and intraperitoneal (*i.p.*) injection respectively, once daily; 2) IM 50 (n=8), IM at 50 mg/kg, oral gavage, once daily; 3) F-AMP 60 (n=8), F-AMP at 60 mg/kg, *i.p.* injection, once daily in the first week, thereafter 5 days on and 2 days off per week; 4) F-AMP 120 (n=8), F-AMP at 120 mg/kg; 5) IM 50 + F-AMP 60 (n=9); 6) IM 50 + F-AMP 120 (n=8). For combination treatments, the dosing schedules are the same as monotherapies. F-AMP was injected immediately after IM administration. Tumor volume and body weight were measured every 2 days. Tumor volume in mm^3 was calculated by the following formula: volume = length × $(width)^2/2$. The day after the last treatment administration, all mice were euthanized and gross necropsies were performed. Tumor tissues were weighed, and portions of tumors were either snap frozen in liquid nitrogen or fixed in 10% neutral buffered formalin and paraffin embedded. Tumor tissues were then subjected to hematoxylin and eosin (H&E) staining and immunohistochemical staining. Three major organs (livers, kidneys and spleens, 6 mice per group) were collected and then subjected to H & E staining for histological analysis.

Immunohistochemical Staining

Sections (4 μm) from formalin-fixed, paraffin-embedded tumor xenografts were subjected to immunohistochemical staining of Ki67, c-KIT and cleaved caspase 3. Briefly, after deparaffinization and rehydration, tissue sections were treated using citrate buffer (pH 6.0) and then hydrogen peroxide (3%). Sections were then incubated with primary antibodies and

then with HRP-labeled polymer antibodies. The staining was visualized by DAB+ (Dako), and nuclei were counterstained with hematoxylin. Photos were captured. Ki67 and cleaved caspase 3 were quantified as the percentage of positive cells in 20 random fields.

Statistics

In vitro data are reported as mean ± SD of 3–5 independent experiments. Values were compared using the Student's *t* test or with one-way ANOVA when three or more groups were present using SigmaPlot software (Systat). *In vivo* data are expressed as mean ± S.E.M. and statistical analyses were carried out with GraphPad Prism 6.0 (GraphPad Software). Two-tailed Student's t test was applied for two-group comparison. A p value less than 0.05 was considered as statistically significant.

RESULTS

High-throughput synergy screening identifies F-AMP as combination agents for GIST therapy

Using a robotic screening system, we exposed GIST-T1, GIST 882, GIST T1-10R cells and the control Hs 919.T cells to the library of FDA-approved drugs in combination with IM. To determine synergistic effects, a combination index was calculated for each drug combination. Seventeen drugs, albendazole, amsacrine, mebendazole, paclitaxel, vinorelbine, dactinomycin, digitoxin, doxorubicin, mitoxantrone, nilotinib, plicamycin, topotecan, auranofin, digoxin, gentian violet, idarubicin, and ouabain, have synergistic effects with IM on GIST-T1 cell proliferation at the indicated concentrations (Supplementary Fig. S1). Sixteen drugs, chloroquine, cladribine, danazol, etoposide, teniposide, clofarabine, daunorubicin, digitoxin, doxorubicin, nilotinib, topotecan, auranofin, carbimazole, ouabain, gentian violet, and idarubicin, have synergistic effects with IM on GIST 882 cell proliferation at the indicated concentrations (Supplementary Fig. S2). Eight drugs, auranofin, bortezomib, carbimazole, digoxin, gentian violet, idarubicin, ouabain and F-AMP, have synergistic effects with IM on GIST T1-10R cell proliferation (Supplementary Fig. S3). Ten drugs (bortezomib, doxorubicin, mitoxantrone, idarubicin HCl, digoxin, daunorubicin, vinorelbine, plicamycin, dactinomycin and mebendazole) failed to show preferential cytotoxicity against GIST cell lines as compared with benign sarcoma Hs 919.T cell line (1). Across all three GIST cell lines, eight drugs showed some degree of synergy with IM, including auranofin, bortezomib, carbimazole, digoxin, gentian violet, idarubicin, ouabain, and F-AMP (FDA-approved drug hits, supplementary Figs. S1–S3).

Combination studies of FDA-approved drug hits with IM in GIST cell lines

To validate the screening result, GIST or the control Hs 919.T cells were treated with eight FDA-approved drug hits alone or in combination with IM using the checkerboard design (Supplementary Fig. S4). Sixty-four different drug concentration combinations were assessed as indicated in Fig. 1. All drugs showed selectively higher growth inhibition on GIST cells compared to Hs 919.T cells (Fig. 1). We have generated the dose-response curves and median-effect plots of IM and FDA-approved drugs in combination to either agent alone. All drugs, but bortezomib, showed a dose-dependent response on GIST cells at the indicated experimental conditions (Supplementary Figs. S5–S12). Median-effect plots

linearize all dose-effect curves that followed the mass-action law principle. The slope calculated by the software (eq.1) (26–28, 30) is then used to generate the normalized isobologram (eq.2, Supplementary Figs. S5–S12). The combination data points in the normalized isobologram figures that fall on the lower-left indicate synergism. Therefore, apparent synergy could be observed in the normalized isobologram plots (Supplementary Fig. S5–S12). To preclude unintended observer bias and to distinguish additive from truly synergism, the Combination Index (CI) model has been employed to evaluate drug interactions, which was originally developed by Chou *et al*. (26–28, 30). The CI method is based on the multiple drug-effect equation of Chou-Talalay, which has been widely used for drug interaction studies (26–28, 30). The CI values were tabulated in Fig. 2. More than 50% of the CI values of idarubicin and carbimazole in combination with IM were less than 1, which indicates synergism. More than 50% of the CI values of digoxin, bortezomib, auranofin, ouabain and gentian violet in combination with IM were greater than 1 and indicate these combinations are antagonistic on the GIST cells (Fig. 2). F-AMP in combination with IM was highly synergistic on the representative GIST lines (95%, 77% and 84% CI values were less than 1 in GIST-T1, GIST 882, and GIST T1-10R cells, respectively) compared to the other seven FDA-approved drug hits (Fig. 2). Based on the well-documented F-AMP (31–34), and its antiproliferative effects on the IM-resistant cells, we chose to further characterize the activity of F-AMP *in vitro* and *in vivo* alone and in combination with IM.

Combination treatment with IM and F-AMP enhances DNA damage in GIST cells

In a previous study, we found that IM treatment alone led to a transient upregulation of p53 and IM-induced DNA damage (15). We speculated that the synergistic activities of IM and F-AMP could be the result of enhanced DNA damage. Therefore, comet assays were used to detect the effects of the combination treatment of IM and F-AMP on double strand DNA breaks in GIST cells. After 3 hours, 2 μmol/L of IM or 10 μmol/L of F-AMP treatment led to significant DNA damage compared with control in GIST-T1 cells (Fig. 3A–C). The combination treatment significantly increased DNA damage by 2.1-fold ($p < 0.05$, grade 3–4) and 4.7-fold ($p < 0.01$, grade 3–4) compared with IM or F-AMP treatment alone, respectively (Fig. 3A–C).

Effect of F-AMP on PI3K, AKT and ERK1/2 pathways in GIST cells

Exposure to IM resulted in dephosphorylation of KIT, AKT and ERK1/2 in GIST cells (1, 18). Our results indicate that F-AMP treatment does not alter the PI3K, AKT and ERK signaling pathways in GIST cells (Fig. 3D). Combined with the comet assay results, our data suggest that the IM treatment both inhibits PI3K, AKT and ERK signaling pathways and induces DNA damage while F-AMP appears to augment DNA damage.

F-AMP alone or in combination with IM induce apoptosis in GIST cells

Given the synergistic interaction we observed between F-AMP and IM in the combination screening, we optimized three combinations that gave the lowest three CI values in each cell line as the optimal doses to evaluate the apoptosis by caspase 3/7 activities (Supplementary Table S1). To examine whether the F-AMP and IM-induced apoptosis in GIST is caspase-

dependent, cells were incubated with optimal doses of the two drugs alone and in combination for 48 hours (Fig. 4A–C) and 72 hours (Supplementary Fig. S5), respectively. In GIST-T1 cell lines, each agent individually as well as combined, induced significant changes in caspase 3/7 activity after 48 hour or 72 hour treatments compared with the vehicle control group (Fig. 4A & Supplementary Fig. S13A). F-AMP and IM, alone and in combination, at a higher concentrations (0.625 μmol/L), induced caspase 3/7 activity in GIST 882 cells after 48 hour or 72 hour treatments compared with the control group (Fig. 4B & Supplementary Fig. S13B). IM alone at the concentrations of 0.078 and 0.313 μmol/L failed to induce caspase 3/7 activity after 48 hour treatments (Fig. 3C). IM treatments did not induce caspase 3/7 activity at the indicated concentrations (0.078 μmol/L or 0.313 μmol/L) after 48 hours or 72 hours in GIST T1-10R cells; F-AMP treatments and the drug combinations did induce significant differences in caspase 3/7 activities compared to IM alone as well as the vehicle control groups (Fig. 4C & Supplementary Fig. S13C). The results confirm that F-AMP as well as the combination of F-AMP and IM induces apoptosis via caspase-dependent signaling pathways in GIST cells, including the IM-resistant cell line. IM does not alter caspase 3/7 activities in IM-resistant GIST T1-10R cells. The apoptotic activities of IM, F-AMP or the drug combination were also evaluated in GIST cells using Annexin V staining. The fraction of early apoptotic cells increased significantly in GIST cells after 48-h treatment at the indicated concentrations (Fig. 4D–F). After treatment, the percentage of Annexin V positive GIST-T1 cells increased by an average of 2.8-fold in IM treatment group (0.313 μmol/L), 3.6 fold in F-AMP treatment group (1.25 μmol/L), and 7.4 fold in the combination treatment group, each relative to the vehicle control group (Fig. 4D). After treatment, the percentage of Annexin V positive GIST 882 cells increased by an average of 2.3-fold in IM treatment group (0.625 μmol/L), 2.4-fold in F-AMP treatment group (2.5 μmol/L), and 6.4-fold in the combination treatment group, each relative to the vehicle control group (Fig. 4E). After treatment, the percentage of Annexin V positive GIST T1-10R cells increased by an average of 2.8-fold in IM treatment group (0.313 μmol/L), 3.6-fold in F-AMP treatment group (0.078 μmol/L), and 4.5-fold in the combination treatment group, each relative to the vehicle control group (Fig. 4F).

F-AMP alone and in combination with IM induces tumor regression in a GIST *in vivo*

To translate the *in vitro* findings described above, we carried out *in vivo* proof of principle studies in a validated mouse model. A xenograft nude mouse model generated by subcutaneous inoculation of GIST-T1 cells was used to examine the anti-tumor effects of IM, F-AMP treatment, each alone and in combination. Based on the previous studies demonstrating that *i.p.* administrations of F-AMP at the dose of 125 mg/kg (once daily, 5 days) and 250 mg/kg (once daily, 3 days) were well-tolerated and led to significant tumor growth suppression in murine models, we chose 60 mg/kg and 120 mg/kg regimens of F-AMP in our study (35–39). F-AMP was administered by *i.p.* injections once daily in the first week, and then 5 days on and 2 days off per week after we observed the body weight loss in the high-dose combination group. After we changed the dosing schedule, the mice in the high dose combination group gained and maintained their body weight throughout the rest of the study (Supplementary Fig. S14). After 73-day treatment, GIST tumor volume decreased by an average of 62% ($p < 0.05$) in IM treatment group (50 mg/kg), 32.1% and 66.3% ($p < 0.01$) in the F-AMP treatment groups (60 or 120 mg/kg respectively), and 76.3% ($p < 0.001$)

and 84.8% ($p < 0.001$) in the IM (50 mg/kg) + F-AMP (60 or 120 mg/kg) groups, each relative to the vehicle-treated control group (Fig. 5A). The paired two-tailed t test showed a significant difference between F-AMP (120 mg/kg) alone and IM + F-AMP (120 mg/kg) treatment groups ($p < 0.05$). IM and high dose of F-AMP (120 mg/kg) alone, as well as the two agents in combination, significantly reduced tumor weights compared to the control group. As shown in Fig. 5B, GIST tumor weight was decreased by an average of 78.6% ($p < 0.05$) in IM group, 37.1% and 72.5% ($p < 0.05$) in F-AMP groups (60 or 120 mg/kg respectively), and 85.7% ($p < 0.05$) and 93.5% ($p < 0.01$) in the IM + F-AMP (60 or 120 mg/kg) treatment groups, each relative to the control group. IM in combination with F-AMP (120 mg/kg) significantly enhanced anti-tumor growth effects compared to IM ($p < 0.05$) or F-AMP (120 mg/kg, $p < 0.01$) treatment alone (Fig. 5B). After 73-day treatment, one mouse was tumor-free in each of the IM, F-AMP (60 mg/kg) and F-AMP (120 mg/kg) alone treatment groups, while two and three mice were tumor-free in IM + F-AMP (60 mg/kg) and IM + F-AMP (120 mg/kg) group, respectively.

The safety profiles of IM, F-AMP alone and in combination were assessed by monitoring body weight and survival of mice in each group. The doses and schedules in the study did not cause discernible adverse effects for monotherapy or combination therapy, as shown by no significant loss of body weight (Supplementary Fig. S14) and no noticeable pathologic changes in the livers, kidneys and spleens among all groups (Supplementary Fig. S15).

IM and F-AMP-mediated tumor growth inhibition correlates with decreased Ki67 and c-KIT expression

To assess the effects of IM and/or F-AMP on tumor morphology, we performed H&E staining, and immunohistochemical staining for Ki67, a proliferation marker, for c-KIT (CD117), a marker for GIST cells, and cleaved caspase 3, an apoptosis marker on tumor sections. H&E staining of tumor sections exhibited enhanced histologic response in treated mice than control mice, except for F-AMP (60 mg/kg) group, as shown by the decrease in cellularity, an increase in stromal fibrosis and the focal areas of necrosis (Fig. 6A). The enhanced histologic response is more evident in combination treatments (Fig. 6A).

Except for the lower F-AMP (60 mg/kg) alone group, GIST-T1 tumors treated with IM and F-AMP alone or in combination, showed a significant decrease in cell proliferation as demonstrated by the significant reduction (23.8%, 28.3%, 24.9% and 58.8%, $p < 0.01$) in Ki67-positive cells in tumors isolated from IM (50 mg/kg), F-AMP (120 mg/kg) and the IM (50 mg/kg) + F-AMP (60 or 120 mg/kg) groups compared with control, respectively (Fig. 5B). In addition, a significant reduction in Ki67-positive cells (29.6%) was observed in IM + F-AMP (60 mg/kg) group when compared with 60 mg/kg F-AMP alone. A decrease in Ki67-positive cells was also observed in IM + F-AMP (120 mg/kg) as compared to the treatment of either drug alone (Fig. 6B).

To further evaluate the therapeutic response to IM and F-AMP, we stained tumor sections for c-KIT expression to assess the number of residual tumor cells present in the specimens. Consistent with the Ki67 staining, the numbers of c-KIT positive cells were lower in IM (50 mg/kg), F-AMP (120 mg/kg) and the IM (50 mg/kg) + F-AMP (60 or 120 mg/kg) groups, as compared to control group (Fig. 6A). The decrease in c-KIT staining, including percentage

of positive cells and staining intensity, was substantially more pronounced in the combination treatment group compared to single agent treatment groups (Fig. 6A).

Tumor apoptosis was examined by staining for the presence of cleaved caspase 3. After the treatment of IM and F-AMP, alone and in combination, tumor tissues showed decreased positive staining for cleaved caspase 3 as compared with control tumors (Fig. 6A & B).

DISCUSSION

Since the FDA approval of IM as a drug treatment for GIST in 2002, the treatment of this sarcoma has radically improved. GIST, resistant to standard chemotherapy and radiation, can now be controlled, at least initially, with IM in the majority of cases. However, these effects are often short-lived, with GISTs demonstrating a median time to progression of approximately two years (12, 16, 21). Therefore, alternative drugs or drugs in combination with IM should be considered for GIST therapy. To accelerate the development of new therapies for GIST patients, we employed an *in vitro* screening approach of FDA-approved drugs to identify drug repurposing opportunities. From the screens of FDA-approved drugs, we identified eight drugs that inhibit GIST cell proliferation alone or in combination with IM. F-AMP showed the highest degree of synergism with IM on GIST cells and was prioritized for further validation because of its efficacy demonstrated in other cancers, the wealth of clinical experience with this agent, and its single agent *in vitro* activity in several GIST cell lines (31–34). Fludara® (Fludarabine Phosphate Injection) has been approved by the FDA for the treatment of patient with B-cell Chronic Lymphocytic Leukemia (CLL) who has not responded to or whose disease has progressed during treatment with at least one standard alkylating-agent containing regimen (FDA). These results are documented in the FDA “rare disease research database” (RDRD), with at least one marketing approval for a common disease indication, for a rare disease indication, or for both common and rare disease indications up through June 2010.

F-AMP inhibits DNA synthesis by interfering with ribonucleotide reductase and DNA polymerase and is being repurposed for different cancers (31–34). This was particularly intriguing given our previous finding in studies to deduce signaling activity in gastrointestinal stromal tumor cell lines treated with IM, in which we applied bioinformatics approaches. We established that IM produced reduced activity in the KIT pathway, as well as unexpected activity in altering the *TP53* pathway (15). Pursuing these findings, we determined that IM-induced DNA damage is responsible for the increased activity of p53, thus identifying a novel off-target activity for this drug. We, therefore, speculated that IM and F-AMP might have both complementary and unique activities in GIST, warranting further clinical investigations. Our study of IM and F-AMP combinations has focused mainly on the question of whether a combination is synergistic rather than simply additive. Synergy could help to define the point at which the unique combination of these agents can provide additional benefit (i.e., improved efficacy with equal or less toxicity) over simply increasing the dose of either agent. Demonstrating synergistic proof of principle preclinically, would then warrant translating these findings to patients.

Our *in vitro* cytotoxicity data showed F-AMP alone potently inhibited GIST cells (1). In the present combination studies, we found that the interaction between IM and F-AMP is highly synergistic in GIST cells. Further validation by western blot showed that F-AMP does not inhibit c-KIT/AKT and MAPK pathways in GIST-T1, GIST 882, and GIST T1-10R cells. However, both F-AMP and IM treatment induce DNA damage, suggesting that the combination of F-AMP with IM increases the growth inhibition effect of GIST cells by synergistically enhance DNA damage. Caspase 3/7 activity analysis and Annexin V staining results suggest that IM and F-AMP in combination and alone induce caspase 3/7 activity and apoptosis in GIST cells. Therefore, the combination of F-AMP and IM represents a promising alternative treatment for imatinib-resistant GIST patients, and warrants clinical evaluation in recurrent GIST.

In agreement with the excellent therapeutic response to IM therapy of GIST patients with exon 11 *KIT* mutations (40, 41), our data employing the mouse xenograft model showed IM (50 mg/kg, orally once daily) profoundly inhibited the growth of GIST-T1 tumor, which contains a primary imatinib-sensitive mutation in *KIT* exon 11. These data are also consistent with the previous reports of the GIST-inhibitory effects of IM in preclinical models (42–45), suggesting our GIST xenograft model was successfully established and reliable.

For the first time, our studies demonstrated that F-AMP alone (120 mg/kg) has substantial anti-GIST activity which is comparable to IM (50 mg/kg) and that the combination of IM and F-AMP (either at 60 or 120 mg/kg) synergistically inhibits tumor growth. Furthermore, advanced GIST progressing on tyrosine kinase therapy frequently have secondary mutations; therefore, there is a rationale for testing combination therapies that target RTK-independent pathways, such as those that block DNA synthesis and lead to enhanced DNA damage. The high degree of synergy observed with the F-AMP/IM combination *in vitro* and *in vivo* in this study provide a strong rationale for considering this combination in patients with GIST.

Supplementary Material

Refer to Web version on PubMed Central for supplementary material.

Acknowledgments

Financial Support: This investigation was supported by grants from the National Cancer Institute (R01 CA106588, awarded to M. von Mehren & A.K. Godwin), the National Institutes of Health (UL1 TR000001-02S1, awarded to A.K. Godwin), the KU Cancer Center's CCSG (P30 CA168524, awarded to A.K. Godwin), National Center for Advancing Translational Sciences (KL2TR000119-04, awarded to Z.Y. Pessetto), and the Kansas Bioscience Authority Eminent Scholar Program (awarded to A.K. Godwin).

We would like to thank the KU Cancer Center's Lead Development and Optimization Shared Resource for providing the drug library and technical support. We would like to acknowledge Marsha Danley (KUH) and Tara Meyer (KUCC's Biospecimen Repository Core Facility) for their support in H&E and IHC staining experiments. The authors would also like to acknowledge support from the University of Kansas Cancer Center, the Kansas Bioscience Authority Eminent Scholar Program, the Chancellors Distinguished Chair in Biomedical Sciences endowment at KUMC, the Ewing Marion Kauffman Foundation, and University of Kansas Endowment Association.

List of Abbreviations

GIST	gastrointestinal stromal tumor
IM	imatinib mesylate
F-AMP	fludarabine phosphate
CI	combination index
CLL	chronic lymphocytic leukemia
RDRD	rare disease research database

References

1. Pessetto ZY, Weir SJ, Sethi G, Broward MA, Godwin AK. Drug repurposing for gastrointestinal stromal tumor. Mol Cancer Ther. 2013; 12:1299–309. [PubMed: 23657945]
2. Weir SJ, DeGennaro LJ, Austin CP. Repurposing approved and abandoned drugs for the treatment and prevention of cancer through public-private partnership. Cancer Res. 2012; 72:1055–8. [PubMed: 22246671]
3. Corless CL, Heinrich MC. Molecular pathobiology of gastrointestinal stromal sarcomas. Annu Rev Pathol. 2008; 3:557–86. [PubMed: 18039140]
4. Hirota S, Isozaki K, Moriyama Y, Hashimoto K, Nishida T, Ishiguro S, et al. Gain-of-function mutations of c-kit in human gastrointestinal stromal tumors. Science. 1998; 279:577–80. [PubMed: 9438854]
5. Heinrich MC, Corless CL, Duensing A, McGreevey L, Chen CJ, Joseph N, et al. PDGFRA activating mutations in gastrointestinal stromal tumors. Science. 2003; 299:708–10. [PubMed: 12522257]
6. Rink L, Godwin AK. Clinical and molecular characteristics of gastrointestinal stromal tumors in the pediatric and young adult population. Curr Oncol Rep. 2009; 11:314–21. [PubMed: 19508837]
7. Corless CL, Barnett CM, Heinrich MC. Gastrointestinal stromal tumours: origin and molecular oncology. Nat Rev Cancer. 2011; 11:865–78. [PubMed: 22089421]
8. Antonescu CR. The GIST paradigm: lessons for other kinase-driven cancers. J Pathol. 2011; 223:251–61. [PubMed: 21125679]
9. Blay JY, von Mehren M, Blackstein ME. Perspective on updated treatment guidelines for patients with gastrointestinal stromal tumors. Cancer. 2010; 116:5126–37. [PubMed: 20661913]
10. Yang J, Du X, Lazar AJ, Pollock R, Hunt K, Chen K, et al. Genetic aberrations of gastrointestinal stromal tumors. Cancer. 2008; 113:1532–43. [PubMed: 18671247]
11. Rink L, Ochs MF, Zhou Y, von Mehren M, Godwin AK. ZNF-mediated resistance to imatinib mesylate in gastrointestinal stromal tumor. PloS one. 2013; 8:e54477. [PubMed: 23372733]
12. Godwin AK. Bench to bedside and back again: personalizing treatment for patients with GIST. Mol Cancer Ther. 2011; 10:2026–7. [PubMed: 22072810]
13. Belinsky MG, Skorobogatko YV, Rink L, Pei J, Cai KQ, Vanderveer LA, et al. High density DNA array analysis reveals distinct genomic profiles in a subset of gastrointestinal stromal tumors. Genes Chromosomes Cancer. 2009; 48:886–96. [PubMed: 19585585]
14. Dupart JJ, Trent JC, Lee HY, Hess KR, Godwin AK, Taguchi T, et al. Insulin-like growth factor binding protein-3 has dual effects on gastrointestinal stromal tumor cell viability and sensitivity to the anti-tumor effects of imatinib mesylate in vitro. Mol Cancer. 2009; 8:99. [PubMed: 19903356]
15. Ochs MF, Rink L, Tarn C, Mburu S, Taguchi T, Eisenberg B, et al. Detection of treatment-induced changes in signaling pathways in gastrointestinal stromal tumors using transcriptomic data. Cancer Res. 2009; 69:9125–32. [PubMed: 19903850]
16. Rink L, Skorobogatko Y, Kossenkov AV, Belinsky MG, Pajak T, Heinrich MC, et al. Gene expression signatures and response to imatinib mesylate in gastrointestinal stromal tumor. Mol Cancer Ther. 2009; 8:2172–82. [PubMed: 19671739]

17. Tarn C, Rink L, Merkel E, Flieder D, Pathak H, Koumbi D, et al. Insulin-like growth factor 1 receptor is a potential therapeutic target for gastrointestinal stromal tumors. Proceedings of the National Academy of Sciences of the United States of America. 2008; 105:8387–92. [PubMed: 18550829]

18. Tarn C, Skorobogatko YV, Taguchi T, Eisenberg B, von Mehren M, Godwin AK. Therapeutic effect of imatinib in gastrointestinal stromal tumors: AKT signaling dependent and independent mechanisms. Cancer Res. 2006; 66:5477–86. [PubMed: 16707477]

19. Tarn C, Godwin AK. The molecular pathogenesis of gastrointestinal stromal tumors. Clinical colorectal cancer. 2006; 6 (Suppl 1):S7–17. [PubMed: 17101067]

20. Tarn C, Godwin AK. Molecular research directions in the management of gastrointestinal stromal tumors. Current treatment options in oncology. 2005; 6:473–86. [PubMed: 16242052]

21. Tarn C, Merkel E, Canutescu AA, Shen W, Skorobogatko Y, Heslin MJ, et al. Analysis of KIT mutations in sporadic and familial gastrointestinal stromal tumors: therapeutic implications through protein modeling. Clinical cancer research: an official journal of the American Association for Cancer Research. 2005; 11:3668–77. [PubMed: 15897563]

22. Frolov A, Chahwan S, Ochs M, Arnoletti JP, Pan ZZ, Favorova O, et al. Response markers and the molecular mechanisms of action of Gleevec in gastrointestinal stromal tumors. Mol Cancer Ther. 2003; 2:699–709. [PubMed: 12939459]

23. Gounder MM, Maki RG. Molecular basis for primary and secondary tyrosine kinase inhibitor resistance in gastrointestinal stromal tumor. Cancer Chemother Pharmacol. 2011; 67 (Suppl 1):S25–43. [PubMed: 21116624]

24. Taguchi T, Sonobe H, Toyonaga S, Yamasaki I, Shuin T, Takano A, et al. Conventional and molecular cytogenetic characterization of a new human cell line, GIST-T1, established from gastrointestinal stromal tumor. Laboratory investigation; a journal of technical methods and pathology. 2002; 82:663–5.

25. Tuveson DA, Willis NA, Jacks T, Griffin JD, Singer S, Fletcher CD, et al. STI571 inactivation of the gastrointestinal stromal tumor c-KIT oncoprotein: biological and clinical implications. Oncogene. 2001; 20:5054–8. [PubMed: 11526490]

26. Chou TC. Drug combination studies and their synergy quantification using the Chou-Talalay method. Cancer Res. 2010; 70:440–6. [PubMed: 20068163]

27. Chou TC. The mass-action law based algorithm for cost-effective approach for cancer drug discovery and development. American journal of cancer research. 2011; 1:925–54. [PubMed: 22016837]

28. Chou TC. Theoretical basis, experimental design, and computerized simulation of synergism and antagonism in drug combination studies. Pharmacological reviews. 2006; 58:621–81. [PubMed: 16968952]

29. Singh NP, McCoy MT, Tice RR, Schneider EL. A simple technique for quantitation of low levels of DNA damage in individual cells. Experimental cell research. 1988; 175:184–91. [PubMed: 3345800]

30. Chou TC, Talalay P. Quantitative analysis of dose-effect relationships: the combined effects of multiple drugs or enzyme inhibitors. Advances in enzyme regulation. 1984; 22:27–55. [PubMed: 6382953]

31. Grever MR, Kopecky KJ, Coltman CA, Files JC, Greenberg BR, Hutton JJ, et al. Fludarabine monophosphate: a potentially useful agent in chronic lymphocytic leukemia. Nouvelle revue francaise d'hematologie. 1988; 30:457–9.

32. Puccio CA, Mittelman A, Lichtman SM, Silver RT, Budman DR, Ahmed T, et al. A loading dose/ continuous infusion schedule of fludarabine phosphate in chronic lymphocytic leukemia. J Clin Oncol. 1991; 9:1562–9. [PubMed: 1714949]

33. Johnson S, Smith AG, Loffler H, Osby E, Juliusson G, Emmerich B, et al. Multicentre prospective randomised trial of fludarabine versus cyclophosphamide, doxorubicin, and prednisone (CAP) for treatment of advanced-stage chronic lymphocytic leukaemia. The French Cooperative Group on CLL. Lancet. 1996; 347:1432–8. [PubMed: 8676625]

34. Marti GE, Stetler-Stevenson M, Grant ND, White T, Figg WD, Tohnya T, et al. Phase I trial of 7-hydroxystaurosporine and fludararbine phosphate: in vivo evidence of 7-hydroxystaurosporine

induced apoptosis in chronic lymphocytic leukemia. Leukemia & lymphoma. 2011; 52:2284–92. [PubMed: 21745173]

35. Hariharan K, Chu P, Murphy T, Clanton D, Berquist L, Molina A, et al. Galiximab (anti-CD80)-induced growth inhibition and prolongation of survival in vivo of B-NHL tumor xenografts and potentiation by the combination with fludarabine. International journal of oncology. 2013; 43:670–6. [PubMed: 23764770]
36. Martiniello-Wilks R, Dane A, Voeks DJ, Jeyakumar G, Mortensen E, Shaw JM, et al. Gene-directed enzyme prodrug therapy for prostate cancer in a mouse model that imitates the development of human disease. The journal of gene medicine. 2004; 6:43–54. [PubMed: 14716676]
37. Martiniello-Wilks R, Wang XY, Voeks DJ, Dane A, Shaw JM, Mortensen E, et al. Purine nucleoside phosphorylase and fludarabine phosphate gene-directed enzyme prodrug therapy suppresses primary tumour growth and pseudo-metastases in a mouse model of prostate cancer. The journal of gene medicine. 2004; 6:1343–57. [PubMed: 15493036]
38. Bagley RG, Roth S, Kurtzberg LS, Rouleau C, Yao M, Crawford J, et al. Bone marrow CFU-GM and human tumor xenograft efficacy of three antitumor nucleoside analogs. Int J Oncol. 2009; 34:1329–40. [PubMed: 19360345]
39. Sorscher EJ, Hong JS, Allan PW, Waud WR, Parker WB. In vivo antitumor activity of intratumoral fludarabine phosphate in refractory tumors expressing E. coli purine nucleoside phosphorylase. Cancer Chemother Pharmacol. 2012; 70:321–9. [PubMed: 22760227]
40. Debiec-Rychter M, Dumez H, Judson I, Wasag B, Verweij J, Brown M, et al. Use of c-KIT/PDGFRA mutational analysis to predict the clinical response to imatinib in patients with advanced gastrointestinal stromal tumours entered on phase I and II studies of the EORTC Soft Tissue and Bone Sarcoma Group. European journal of cancer. 2004; 40:689–95. [PubMed: 15010069]
41. Heinrich MC, Corless CL, Demetri GD, Blanke CD, von Mehren M, Joensuu H, et al. Kinase mutations and imatinib response in patients with metastatic gastrointestinal stromal tumor. J Clin Oncol. 2003; 21:4342–9. [PubMed: 14645423]
42. Rossi F, Yozgat Y, de Stanchina E, Veach D, Clarkson B, Manova K, et al. Imatinib upregulates compensatory integrin signaling in a mouse model of gastrointestinal stromal tumor and is more effective when combined with dasatinib. Molecular cancer research: MCR. 2010; 8:1271–83. [PubMed: 20736294]
43. Smyth T, Van Looy T, Curry JE, Rodriguez-Lopez AM, Wozniak A, Zhu M, et al. The HSP90 inhibitor, AT13387, is effective against imatinib-sensitive and -resistant gastrointestinal stromal tumor models. Mol Cancer Ther. 2012; 11:1799–808. [PubMed: 22714264]
44. Floris G, Sciot R, Wozniak A, Van Looy T, Wellens J, Faa G, et al. The Novel HSP90 inhibitor, IPI-493, is highly effective in human gastrostrointestinal stromal tumor xenografts carrying heterogeneous KIT mutations. Clinical cancer research: an official journal of the American Association for Cancer Research. 2011; 17:5604–14. [PubMed: 21737509]
45. Floris G, Debiec-Rychter M, Wozniak A, Stefan C, Normant E, Faa G, et al. The heat shock protein 90 inhibitor IPI-504 induces KIT degradation, tumor shrinkage, and cell proliferation arrest in xenograft models of gastrointestinal stromal tumors. Mol Cancer Ther. 2011; 10:1897–908. [PubMed: 21825009]

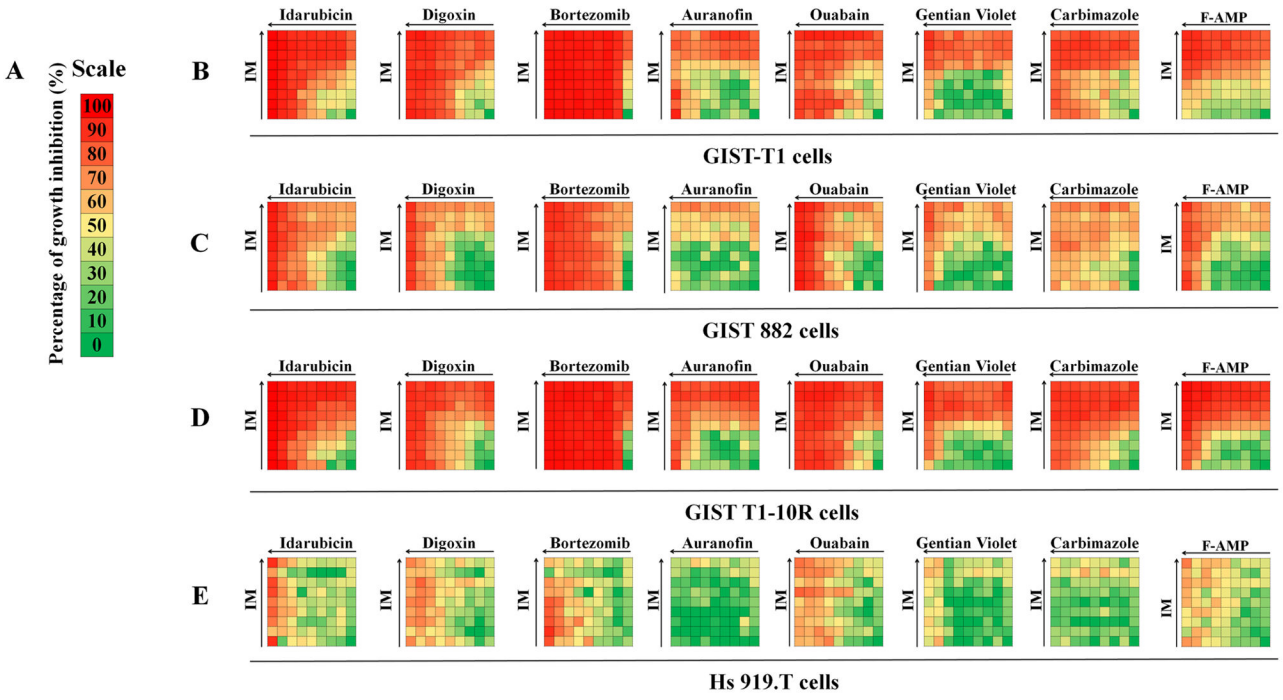

Figure 1.

Drug interaction signatures for GIST and benign osteoma cell lines representing all combinatorial data compiled in a 9 by 9 drug matrix. Cells were treated with vehicle, FDA-approved drug, IM or the drug combination for 72 h. A) Color scale for percentage of the inhibition values of cell proliferation. Synergistic antiproliferative effects of FDA-approved drugs and IM in cells were assessed by CellTiter Glo assay in B) GIST-T1, C) GIST 882, D) GIST T1-10R cells, and in E) Hs. 919.T, a benign osteoid osteoma cell line (as a non-malignant control) at 64 different drug ratios (concentrations range from 7.8 nmol/L to 1 μmol/L, half-dilutions for each drug). Right columns represent IM treatment alone and bottom rows represent FDA-approved drug treatment alone. Arrows indicate the increasing concentrations of each drug.

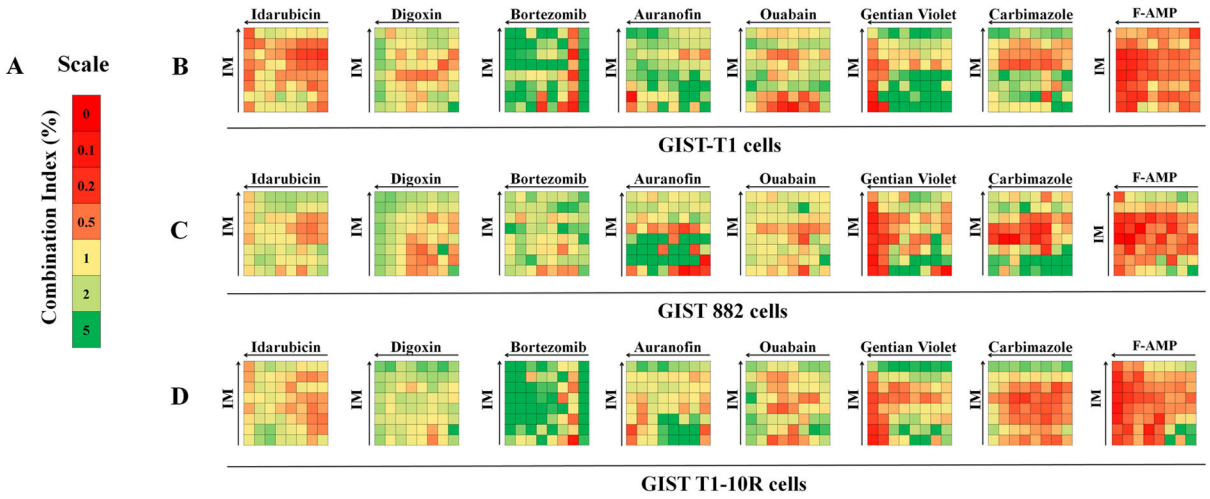

Figure 2.

CI value analysis. A) Color scale for CI values. B) GIST-T1, C) GIST 882, and D) GIST T1-10R cells were treated with vehicle, FDA-approved drug, IM or the drug combination for 72 h. Synergy between drugs and IM was tested by CellTiter Glo assay in three GIST cell lines at 64 different drug ratios (concentrations range from 7.8 nmol/L to 1 μmol/L, half-dilutions for each drug). Arrows indicate the increasing concentrations of each drug.

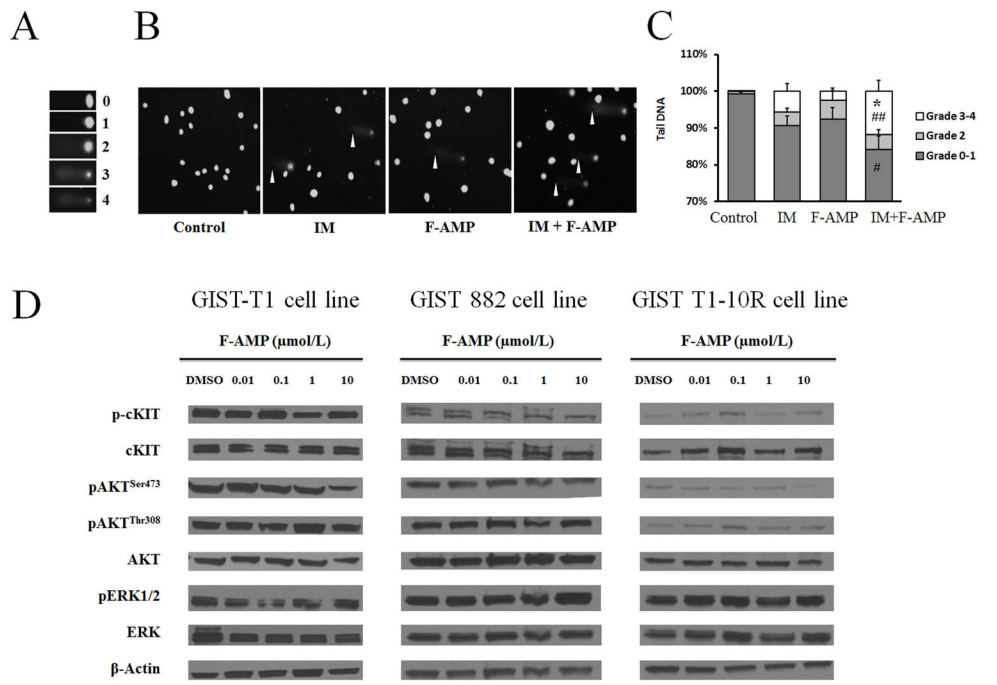

Figure 3.

Effect of F-AMP on GIST cells. IM in combination with F-AMP enhances DNA damage in GIST-T1 cells. A) Grading of comet cells. B) Representative images showing DNA damage in GIST-T1 cells induced by IM (2 µmol/L, 3 hours), F-AMP (10 µmol/L, 3 hours) alone or in combination. White arrowheads indicate comet tails. Magnification, 100X. C) Quantitative DNA damage induced by IM, F-AMP treatment alone or in combination, as shown by tail DNA %. Tail DNA% was defined as 100 × Tail DNA intensity/Cell DNA intensity, and was used for grading. At least 150 cells in 20 randomly selected fields per slide were graded. Data are expressed as mean ± S.D. of three independent experiments. *$p < 0.05$, IM+F-AMP vs. IM; $^{\#}p < 0.05$, $^{\#\#}p < 0.01$, IM+F-AMP vs. F-AMP. D) F-AMP does not affect KIT protein levels or downstream signaling effectors. GIST-T1, GIST 882, and GIST T1-10R cells were treated with or without F-AMP for 6 h and whole-cell extracts were analyzed by western blotting with the indicated antibodies.

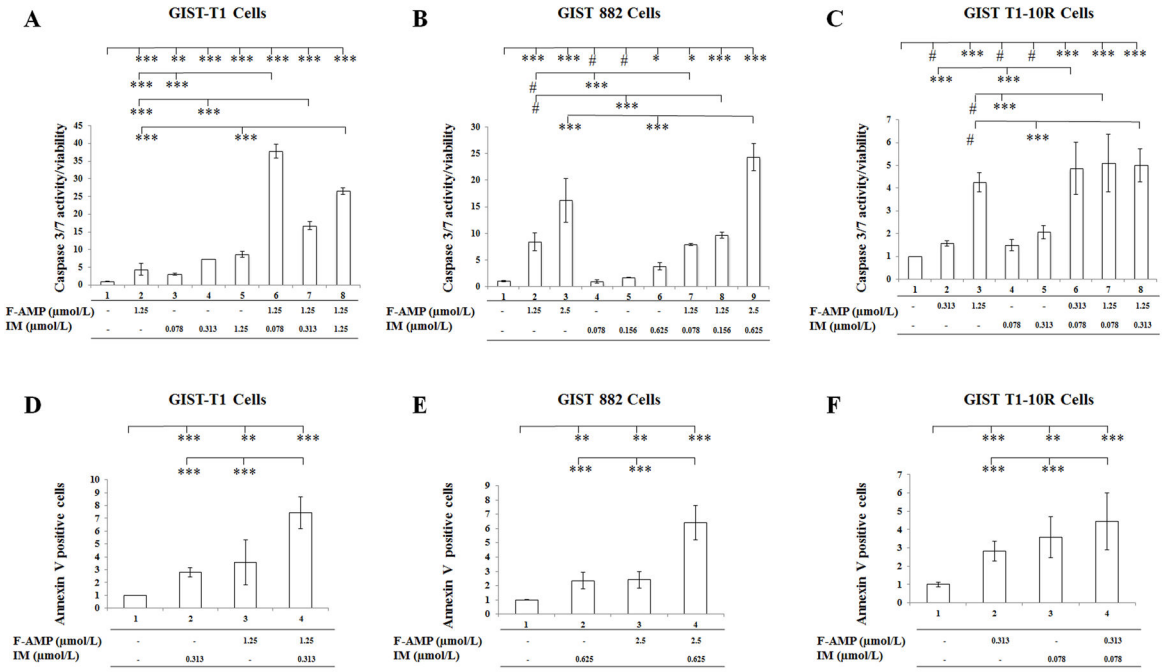

Figure 4.

Apoptosis analysis of GIST cells treated with vehicle, F-AMP, IM, or the drug combination. Assays were evaluated at 48 hours post drug treatment at the optimal doses. A, B and C) F-AMP, IM and the drug combination treatments induce caspase 3/7 activity in GIST cells. D, E, and F) F-AMP, IM and the drug combination treatments induce early apoptosis (annexin V staining) in GIST cells. Data are expressed as mean ± S.D. # $p > 0.05$, * $p < 0.05$, ** $p < 0.005$, *** $p < 0.001$.

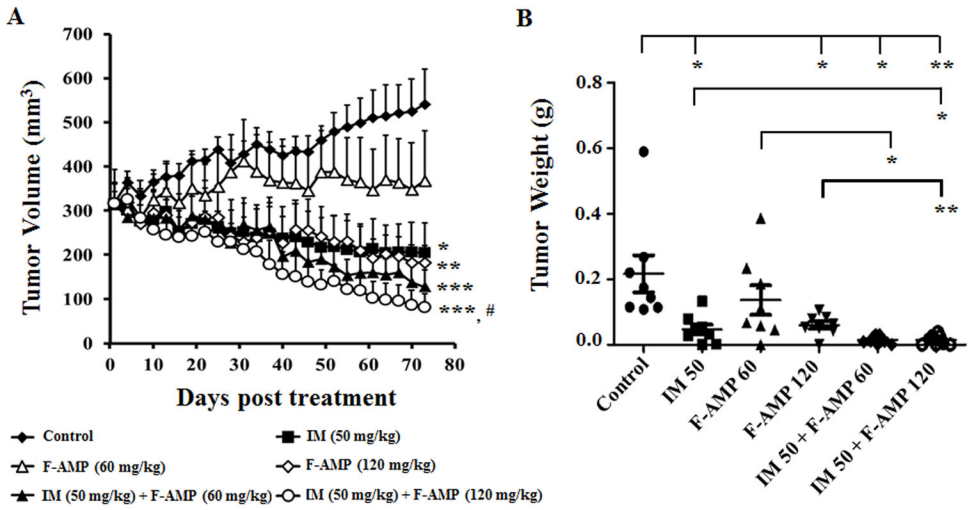

Figure 5.

Synergistic anti-tumor effects of IM in combination of F-AMP against GIST in a xenograft nude mouse model. Ncr nu/nu mice were s.c. injected with 3×10^6 GIST-T1 cells. After tumor volume reached approximately 316 mm^3 on average, mice were randomized into groups treated with vehicle (saline and 5% DMSO), IM (50 mg/kg), F-AMP (60 or 120 mg/kg) or IM (50 mg/kg) + F-AMP (60 or 120 mg/kg) for 73 days. Tumor volumes were measured every 2 days. After 73-day treatment, mice were euthanized and the tumors were weighed. A) Inhibition of tumor growth in mice by IM, F-AMP treatment alone or in combination. Data are expressed as mean ± S.E.M. * $p < 0.05$, ** $p < 0.01$, *** $p < 0.001$, *vs*. control; $^{\#}$ $p < 0.05$, *vs*. F-AMP 120 mg/kg. B) Dot plot of tumor weights from each treatment group. The number of tumor-free mouse was measured in controls (n=0) and IM 50 (n=1), F-AMP 60 (n=1), F-AMP 120 (n=1), IM 50 + F-AMP 60 (n=2), and IM 50 + F-AMP 120 (n=3) treated groups. Data are expressed as mean ± S.E.M. * $p < 0.05$, ** $p < 0.01$.

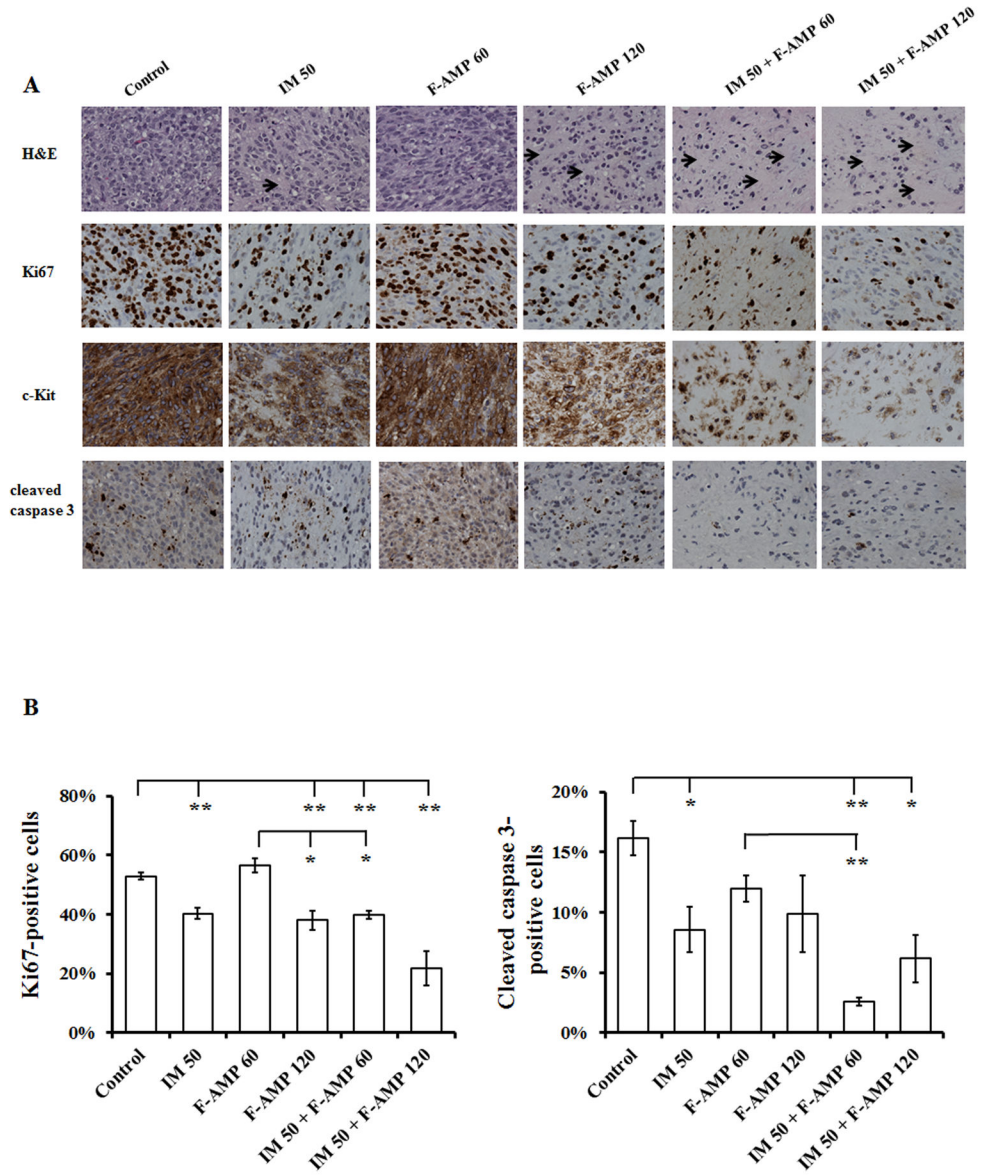

Figure 6.

IM in combination of F-AMP significantly inhibits Ki67 and c-KIT expression in GIST-T1 tumor xenografts. Tumors were collected on the day after the last treatment and were then subjected to H&E staining and immunohistochemical detection of Ki67, c-KIT and cleaved caspase 3 expression. A) Representative images of H&E staining and immunohistochemical staining of Ki67, c-KIT and cleaved caspase 3 in mice tumors. Arrows indicate the decrease in cellularity and the increase in stromal fibrosis. Magnification, 400X. B) Quantification of Ki67 and cleaved caspase 3 in each treatment group. Positive stained cells are brown and all nuclei are counterstained light blue. The percentage of positive nuclei relative to total nuclei was assessed from 20 randomly selected fields of each sample. Data are represented as mean ± S.E.M. n=2–4, * $p < 0.05$, ** $p < 0.01$.